

Article

Methyltrioctylammonium Octadecanoate as Lubricant Additive to Different Base Oils

Javier Faes ¹, Rubén González ¹, David Blanco ², Alfonso Fernández-González ³, Antolin Hernández-Battez ², Patricia Iglesias ⁴ and José Luis Viesca ^{2,*}

¹ Department of Marine Science and Technology, University of Oviedo, 33203 Gijón, Spain; faesjavier@uniovi.es (J.F.); gonzalezrruben@uniovi.es (R.G.)

² Department of Construction and Manufacturing Engineering, University of Oviedo, 33203 Gijón, Spain; blancoadavid@uniovi.es (D.B.); aehernandez@uniovi.es (A.H.-B.)

³ Department of Physical and Analytical Chemistry, University of Oviedo, 33006 Oviedo, Spain; fernandezgalfonso@uniovi.es

⁴ Rochester Institute of Technology, Kate Gleason College of Engineering, Rochester, NY 14623, USA; pxieme@rit.edu

* Correspondence: viescajose@uniovi.es; Tel.: +34-98-545-80-44

Abstract: This study investigates the use of an ionic liquid obtained from fatty acids (FAIL) as an additive at 2 wt.% in two different base oils: a mineral oil (M1) and a polyol ester (E1). Physicochemical characterization of the base oil–FAIL blends confirmed the miscibility of the FAIL in the base oils. The addition of the FAIL hardly changed the density of the base oils and the viscosity slightly increased at lower temperatures. The tribological performance of the base oils and their blends with the FAIL was determined using three different tests: Stribeck curve determination and tribofilm formation tests, both under sliding/rolling motion, and reciprocating wear tests. The M1 + FAIL blend showed the lowest friction values under the mixed lubrication regime due to its higher viscosity, while the E1 + FAIL showed the lowest friction values under the elastohydrodynamic lubrication regime, which may well have been due to its higher polarity. Only the E1 + FAIL blend outperformed the antiwear behavior of the base oil, probably because it has better chemical affinity (higher polarity) for the metallic surface. SEM images showed that the predominant wear mechanism was adhesive-type with plastic deformation and XPS studies proved that the presence of increasing amounts of organic oxygen on the wear scar caused better antiwear performance when the E1 + FAIL blend was used.

Keywords: fatty acid ionic liquid; lubricant additive; miscibility; friction; wear



Citation: Faes, J.; González, R.; Blanco, D.; Fernández-González, A.; Hernández-Battez, A.; Iglesias, P.; Viesca, J.L. Methyltrioctylammonium Octadecanoate as Lubricant Additive to Different Base Oils. *Lubricants* **2022**, *10*, 128. <https://doi.org/10.3390/lubricants10060128>

Received: 27 May 2022

Accepted: 15 June 2022

Published: 17 June 2022

Publisher's Note: MDPI stays neutral with regard to jurisdictional claims in published maps and institutional affiliations.



Copyright: © 2022 by the authors. Licensee MDPI, Basel, Switzerland. This article is an open access article distributed under the terms and conditions of the Creative Commons Attribution (CC BY) license (<https://creativecommons.org/licenses/by/4.0/>).

1. Introduction

Ethylammoniumnitrate [(C₂H₅)NH₃] [NO₃] was reported more than 100 years ago as a liquid salt, and this moment could be considered as the birth of the so-called ionic liquids [1]. Research into these special salts, with melting points lower than 100 °C, gained attention again in the 1970s with the utilization of pyridinium/imidazolium cations and halide/halogen aluminate anions as electrolytes in batteries [2,3]. The issue regarding the possible basicity or acidity of ILs was solved in the 1990s when Wilkes and Zawarotko [4] employed neutral weakly coordinating anions, such as tetrafluoroborate [BF₄][−] and hexafluorophosphate [PF₆][−], to obtain ILs. Since then, these novel substances have become important in different industrial applications, such as catalysts, liquid crystals, extraction technology, solvents and lubrication [5–9].

Research into the use of ILs in lubrication began in 2001 [9], mainly due to some of their excellent physicochemical properties (e.g., wide liquid range, low volatility, etc.), which are important for formulated lubricants. The number of studies on this topic has increased enormously since 2001, showing the great interest these novel substances attract within the lubrication field [10–20]. It is the tribofilm-forming capacity of these ionic compounds that is mainly responsible for both the friction and wear reduction [21–30].

However, though ILs were shown to have special properties, certain problems were also found regarding their use in lubrication. Firstly, the majority of ILs contain toxic or hazardous elements that are potentially harmful to the environment (e.g., halogens and/or heavy metals) [31–35]. Therefore, if ILs are to be considered as “green compounds”, properties such as their toxicity and biodegradability must be controlled. Secondly, since the price of ILs remains high, their use as neat lubricants is limited to severe conditions, such as high temperature, load and vacuum [36–41]. Due to these limitations, the main application of ILs in lubrication is currently as lubricant additives [25,42–51].

Some lubrication research found that additizing non-polar oils (mineral or polyalphaolefin) with a polar additive at low concentration could improve the adsorption of the former on metallic surfaces due to the polar nature of these substances [52–54]. Taking this phenomenon into account, several studies have been published employing ILs as a lubricant additive at low concentrations in non-polar oils, forming base oil–IL emulsions or unstable base oil–IL blends [55–59]. Attempting to overcome the miscibility problem, some authors found that ILs display better compatibility with polar oils [51,60–71]. However, some phosphonium cation-based ILs were also found to be miscible in non-polar oils [44,46,47].

The increase in social awareness of the global environmental problems caused by human activity has brought a need to find new lubricants to help confront the growing effects of pollution on the environment [72–74]. To find these new, environmentally friendly compounds, the toxicity problems of ILs have been addressed by selecting more appropriate constituent ions [75–78]. One group of these novel compounds are fatty acid anion-based ionic liquids (FAILs), obtained via metathesis and first reported in 2013 [79]. Currently, research into the use of FAILs in lubrication keeps expanding [80–96] and it constitutes a hot research topic. In this study, one novel FAIL (methyltrioctylammonium octadecanoate or $[N_{8,8,8,1}][C_{18:0}]$), synthesized from natural sources, was tribologically characterized as a lubricant additive for the first time in two different base oils (synthetic ester and mineral oil). The $[N_{8,8,8,1}][C_{18:0}]$ was selected as a neat sample considering the following properties: no corrosion activity on steel [97] and high thermal stability [98].

2. Materials and Methods

2.1. Ionic Liquid and Base Oils

The fatty acid anion-based ionic liquid methyltrioctylammonium octadecanoate ($[N_{8,8,8,1}][C_{18:0}]$) was synthesized following a three-step process (ester formation, salt metathesis reaction and the elimination of solvent), as described in previous work [99]. Stearic acid (natural >98%) and methyltrioctylammonium bromide ionic liquid ($[N_{8,8,8,1}][Br]$) (>97%) were used as anion and cation precursors, respectively. Sodium hydroxide, toluene (99.8%) and ethanol solution (70% *w/w*), provided by Sigma-Aldrich Corporation. (St. Louis, MO, USA) were employed without further purification as chemical reagents for the synthesis.

The molecular structure of this new FAIL was previously identified using Fourier-transform infrared spectroscopy (FTIR) with a Varian 670-IR from Agilent Technologies (Santa Clara, CA, USA) and nuclear magnetic resonance (NMR) analysis using a Bruker serie Avance AV600 from Bruker Corporation (Billerica, MA, USA) [87]. In addition, some of its properties (water solubility, viscosity, viscosity index and refractive index) were correlated with its bacterial toxicity and biodegradability [92]. Its corrosion and tribological performance as a pure lubricant were also investigated [97]. The chemical structure and the empirical formula of the methyltrioctylammonium octadecanoate ($[N_{8,8,8,1}][C_{18:0}]$) ionic liquid are shown in Figure 1.

Additionally, two different base oils, kindly supplied by REPSOL S.A. (Madrid, Spain), were used: a mineral base oil (SN-150), coded M1; and a polyolester base oil (Priolube 3970), coded E1. These base oils were selected among those where the ionic liquid was soluble.

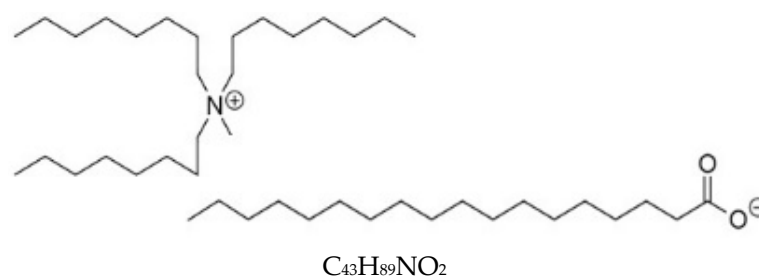


Figure 1. Chemical structure and empirical formula of the $[N_{8,8,8,1}] [C_{18:0}]$ FAIL.

2.2. Blend Characterization: Miscibility, Viscosity and Density

In order to confirm the miscibility of this novel FAIL in the base oils mentioned above, solubility tests at 0.5, 1 and 2 wt.% were performed in each of the base oils, using an ultrasonic probe Bandelin Sonopuls HD2200 from Bandelin Electronics (Berlin, Germany) at 70% amplitude for 5 min and maintaining the blend temperature below 60 °C. Later, the miscibility of the blends was measured with the light backscattering technique in a Turbiscan aging station from Formulacion (Toulouse, France). These tests were conducted at 30 °C for 14 days, taking measurements every 24 h to study possible phase separation.

The dynamic viscosity and density of the blends were measured at atmospheric pressure according to ASTM D7042 over a temperature range of 20–100 °C using a Couette rotational viscometer Stabinger Viscometer SVM3001 from Anton Paar GmbH (Graz, Austria).

2.3. Tribological Tests

Tests were carried out to study the tribological behavior of the $[N_{8,8,8,1}] [C_{18:0}]$ FAIL as an additive in two base oils. Firstly, two independent tests were performed using a Mini Traction Machine tribometer (MTM2), from PCS Instruments (London, UK) with a ball-on-disk configuration (Figure 2). The first test was undertaken at constant values for the load, slide-to-roll ratio (SRR) and temperature, while friction was measured over a speed range to obtain the so-called Stribeck curve. This procedure was repeated for four temperatures in a single test, allowing the behavior of the blends to be studied under different lubrication regimes. In order to study tribofilm formation due to the interaction between the lubricant and the surface, a second test in the MTM2 was performed where the load, speed, temperature and SRR were kept constant during tests and the ball was periodically halted, separated from the contact and loaded against a coated glass disc. Then, the thickness of the tribofilm formed on the ball's surface was measured by optical interferometry. The methodology employed was described in [100].

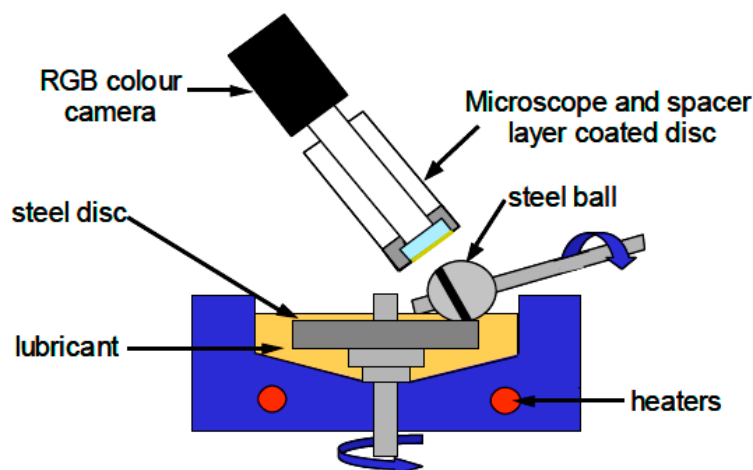


Figure 2. Schematic diagram of the configuration used for the Stribeck curve determination.

Table 1 shows the test conditions employed in the two abovementioned experiments. In all of them, AISI 52,100 steel balls ($R_a < 0.02 \mu\text{m}$, diameter of 19.05 mm and 800–920 HV) and discs ($R_a < 0.02 \mu\text{m}$, diameter of 46 mm and 720–780 HV) were used as specimens and supplied by PCS Instruments (London, UK). The steel ball was loaded against the steel disc submerged in 10 mL of the lubricant. Previously, both specimens were cleaned in an ultrasonic bath with heptane for 15 min, then washed with ethanol and finally dried with hot air.

Table 1. Test conditions of the experiments conducted in the mini traction machine.

	Load (N)/Max. Contact Pressure (GPa)	Main Entrainment Speed ^a ($\text{mm}\cdot\text{s}^{-1}$)	Slide-to-Roll Ratio ^b (%)	Temperature ($^{\circ}\text{C}$)
Stribeck measurement	30/0.95	2500 to 10 ^c	50	40, 60, 80, 100
Film formation measurement	50/1.13	150	50	100

^a Mean entrainment speed can be defined as $(u_d + u_b)/2$, where u_d and u_b are the lineal velocity of the disk and the ball at the point of contact, respectively. ^b Slide-to-roll ratio was calculated as $100 \times 2(u_d - u_b)/(u_d + u_b)$. ^c Steps of $100 \text{ mm}\cdot\text{s}^{-1}$ from 2500 to 100 and steps of $10 \text{ mm}\cdot\text{s}^{-1}$ from 100 to 10.

Additionally, accelerated friction and wear tests were carried out in a Bruker UMT-3 tribometer from Bruker Corporation (Billerica, MA, USA) using a reciprocating ball-on-disc configuration (Figure 3). AISI 52,100 steel balls ($R_a = 0.05 \mu\text{m}$, diameter of 6 mm and 58–66 HRC) and discs ($R_a = 0.018 \mu\text{m}$, diameter of 10 mm and 225 HV) were also employed in this case. Thirty-minute experiments with the presence of 4 mL of lubricant sample were performed at a 50 N-load (medium contact pressure of 1.63 GPa), 15 Hz frequency, 100°C , 4 mm stroke length and relative humidity within the 40–60% range. The expected lubrication regime was mixed. During the experiments, the coefficient of friction was recorded. To obtain statistically acceptable results, three repetitions of each test were performed. The samples were cleaned before each test following the procedure previously described for the Mini Traction Machine experiments. At the end of these tests, the wear volume on the disk was determined by using a Leica DCM 3D confocal microscope from Leica Microsystems GmbH (Wetzlar, Germany).

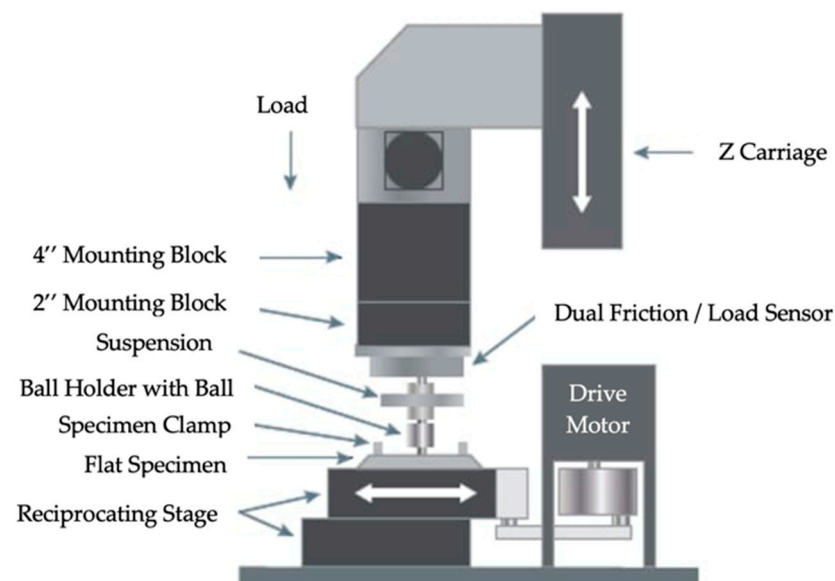


Figure 3. Configuration of the tribological tests conducted in the UMT-3 tribometer.

2.4. Surface Analysis

In order to identify the predominant wear mechanism, after the wear test in the UMT-3 tribometer, the worn surface on the disk was analyzed by Scanning Electron Microscopy

(SEM) and Energy Dispersive X-ray spectroscopy (EDX). A JSM 5600 SEM from JEOL Ltd. (Tokyo, Japan) instrument with an X-ray energy-dispersive microanalyser model Inca Energy 200 from Oxford Instruments (Abingdon, UK) was used for secondary electron imaging (SEI), with an accelerating voltage of 20 kV.

Additionally, possible tribochemical interactions between lubricant mixtures and surfaces were studied using X-ray photoelectron spectroscopy (XPS). Tests were conducted with a PHI VersaProbe II spectrometer from Physical Electronics (Chanhassen, MN, USA), using a monochromatized $K\alpha(\text{Al})$ X-ray source (1486.7 eV, 4.8 W) for the experiments. The final X-ray spot (diameter $20\ \mu\text{m}^2$) was always focused on the wear scar. Adventitious carbon at 284.6 eV was selected to correct binding energies. Pass energy was selected in the 30–60 eV range. The total number of scans depended on each sample and element.

3. Results and Discussion

3.1. Miscibility, Viscosity and Density Values

The FAIL was miscible in both base oils for all concentrations. Figure 4 shows the results of the miscibility tests for the 2 wt.% concentration and the measurements of light backscattering at 0, 7 and 14 days, confirming the absence of phase separation in the base oil + FAIL blends.

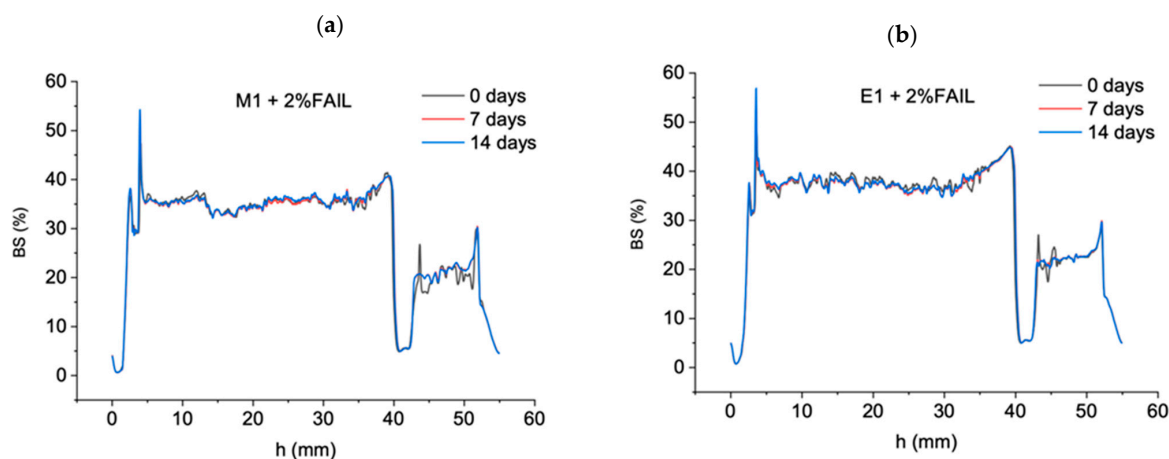


Figure 4. Stability of the blends measured by light backscattering technique (a) M1 + 2%FAIL, (b) E1 + 2%FAIL.

Figure 5 shows density and kinematic viscosity values obtained for the different base oils and their mixtures with the FAIL. As can be seen, the density of the base oils hardly changed with the addition of FAIL. The ester base oil (E1), pure or mixed with the FAIL, showed the highest density values, followed by the mineral oil (M1). Regarding the kinematic viscosity, it can be observed for both base oils that the addition of 2 wt.% of FAIL slightly increased the viscosity value, particularly at lower temperatures.

3.2. Tribological Tests

Figure 6 shows traction coefficient results versus mean entrainment speed (Stribeck curves) for the test conducted with all the lubricants at 40, 60, 80 and 100 °C. As expected, the change from an elastohydrodynamic lubrication (EHL) regime to a mixed lubrication (ML) regime occurred at a higher speed with increasing temperature. Under the EHL regime the M1 base oil, with and without FAIL, exhibited the highest traction coefficient values, which was related to their having the highest viscosity among the lubricant samples. No important differences in friction value could be observed under this regime (speed > 100 mm/s) between base oils and their corresponding mixtures with the ionic liquid, except for the E1 base oil at high temperatures, where the presence of FAIL caused an increase in friction value.

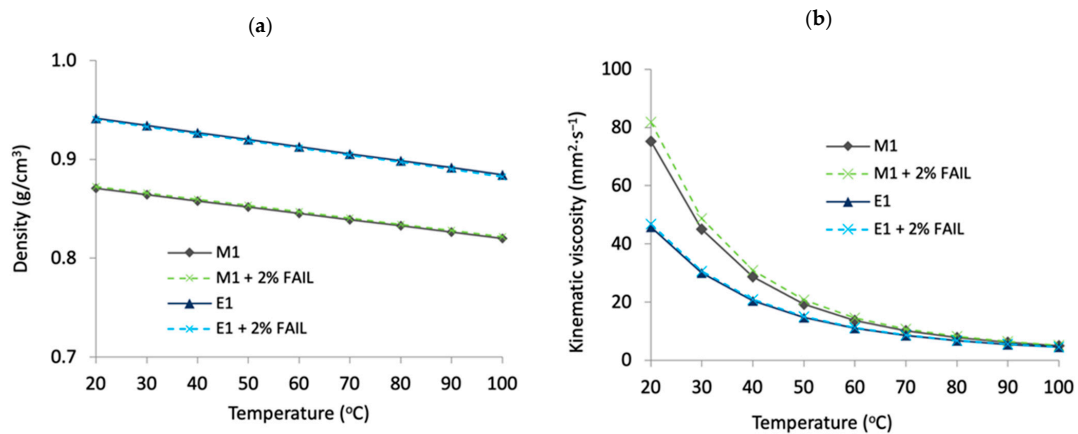


Figure 5. (a) Density and (b) kinematic viscosity values of the lubricant samples.

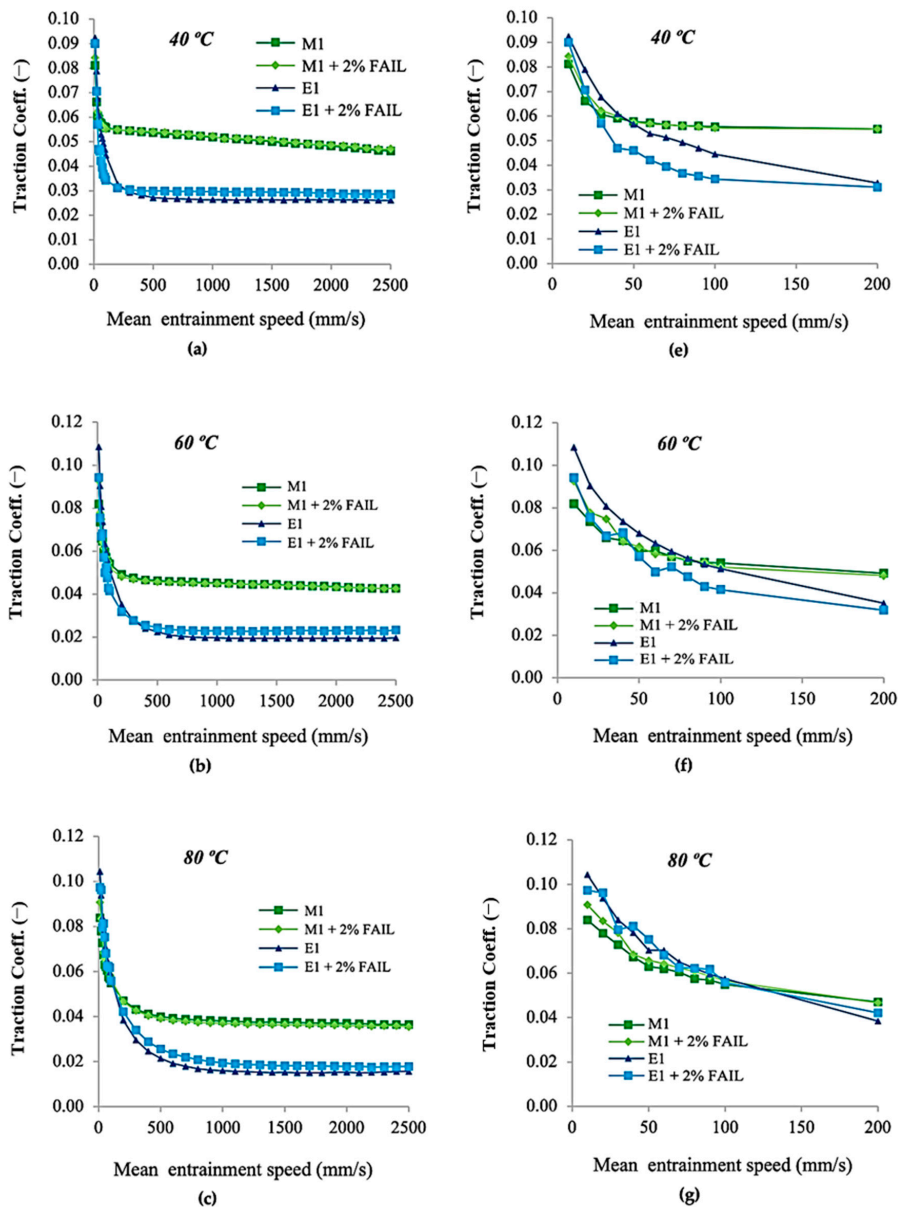


Figure 6. Cont.

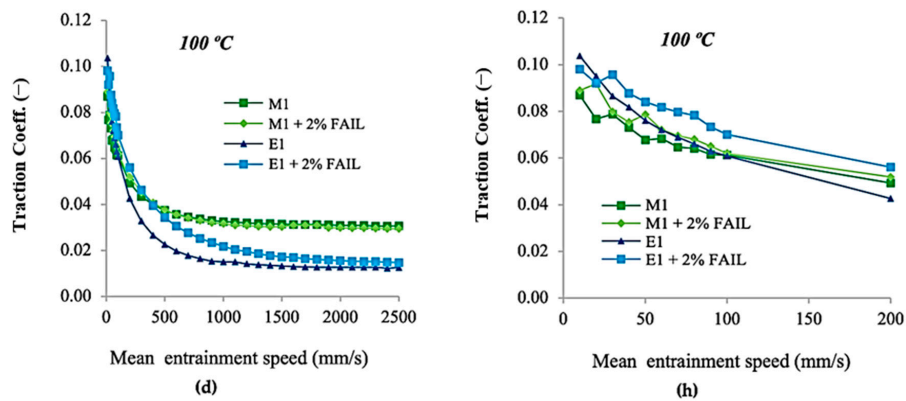


Figure 6. Traction coefficient values from the (a–d) Stribeck curve tests and (e–h) magnification of the 10–200 mm/s speed range.

On the other hand, under the ML regime (speed of 100 mm/s and below), the friction results were more related to the asperities contact phenomenon. However, in general, the M1 base oil and its mixture with FAIL showed lower friction values, especially at higher temperatures, due to their higher viscosity, which facilitates the formation of a thicker lubricant film.

The tribofilm formation on the balls used in the second kind of test carried out in the MTM2 is shown in Figure 7. A color change (from blue to brown) can be seen on the surfaces of the balls and is indicative of layer formation during the tests.

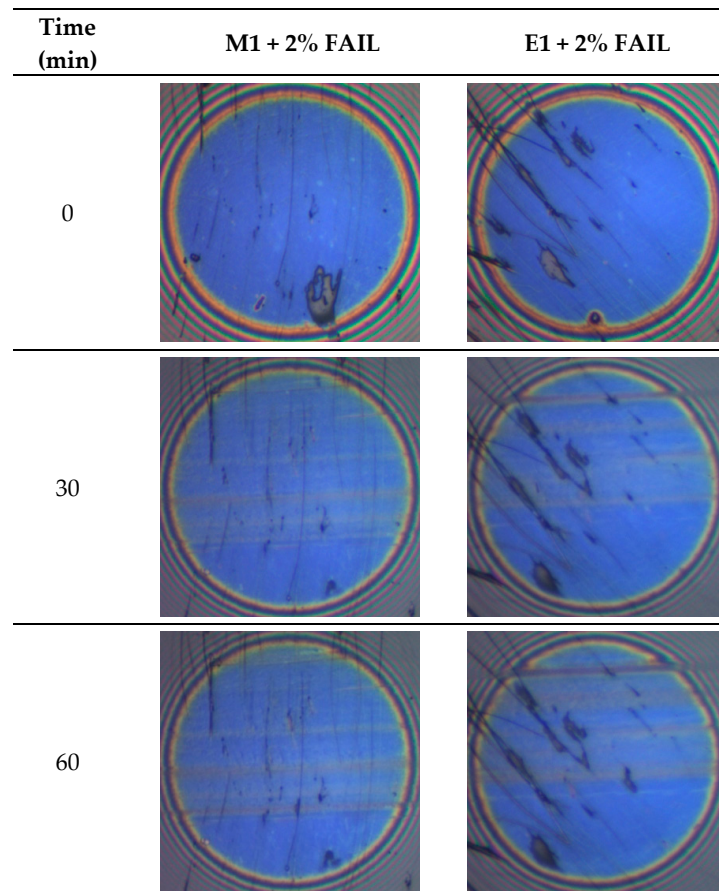


Figure 7. Interference images of tribofilm formation on ball surfaces at 0, 30 and 60 min.

The thickness of the tribofilm formed on the balls during tests with all lubricants can be observed in Figure 8. In agreement with the abovementioned results, there was an increase in the E1 + FAIL tribofilm thickness during the test, which achieved the highest values recorded for the two lubricant samples studied. The fluctuations in the film thickness may have been related to the coexisting formation/wear processes that took place during the test. On the other hand, the M1 + FAIL registered only a very slight increase in tribofilm thickness, probably due to its high viscosity, which prevents greater interaction between the FAIL and the surface.

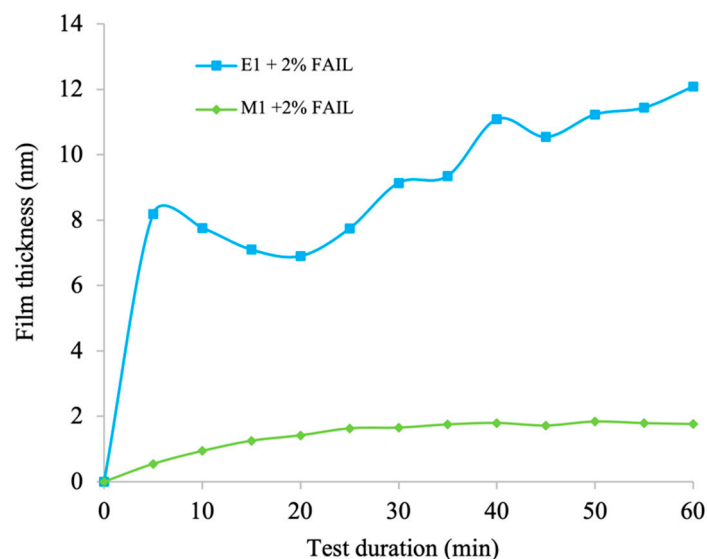


Figure 8. Thickness of tribofilm formed on the ball surfaces.

Figure 9 shows the mean values for the coefficient of friction (COF) in the reciprocating tests carried out at 100 °C. These friction values are characteristic of a mixed lubrication regime. Analogously to the results obtained in previous works where other FAILs of the same family were studied [88,96], the addition of 2% of FAIL to a lubricating base oil did not significantly modify its friction behavior. However, while in the previous studies the COF increased slightly with the additivation, in the present work the addition of FAIL caused, in both cases, a slight decrease in COF. This favorable differential behavior could be attributable to the higher thermal stability of the studied FAIL [98], which is related to its longer alkyl chain length.

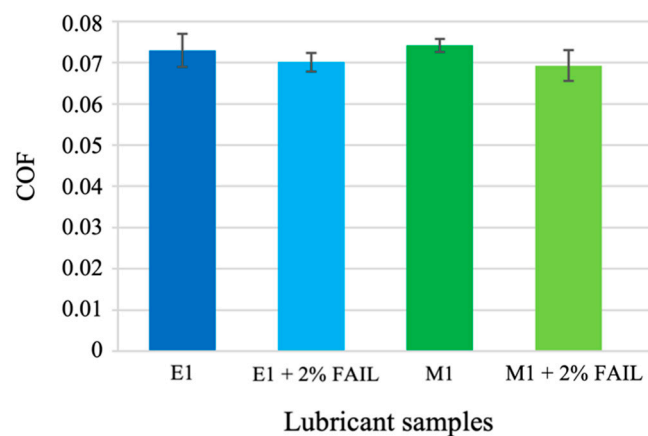


Figure 9. Average COF values after tests at 100 °C.

Figure 10 shows the wear volume on the disc from wear tests at 100 °C. The E1 + FAIL blend achieved a notable reduction in wear compared to the base oil without additives. This

behavior was probably related to its better chemical affinity with the metallic surface due to its having both higher polarity [53,54,88] and affinity for the metal surfaces. However, the antiwear behavior of the blend with the base oil M1 at 100 °C worsened, probably due to the lower polar nature of mineral oils. This could be attributed to the dynamic of the wear process, where differences in the rate of formation and destruction of the tribolayer in the contact can lead to wear increases.

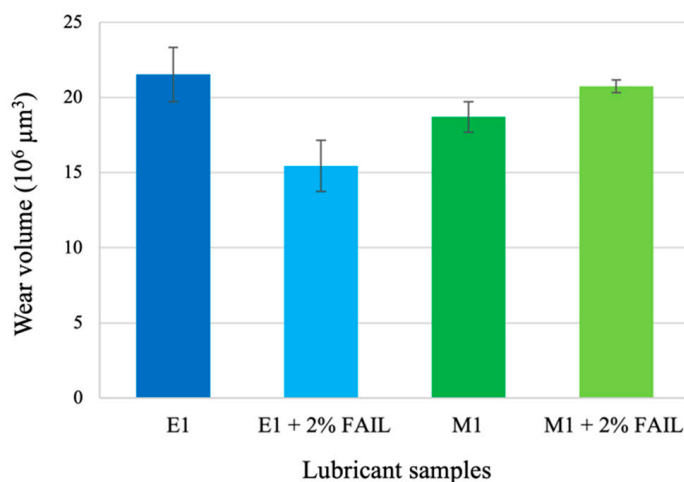


Figure 10. Wear volume of the discs after tests at 100 °C.

3.3. Surface Analysis

The wear scar on the disc after reciprocating wear tests was studied with an SEM technique and the predominant wear mechanism found was of the adhesive type with plastic deformation, which is usually found under mixed lubrication regimes (Figure 11). The state of the worn surface shows that the addition of FAIL to the E1 base oil caused a clear decrease in the scar width. These results are in agreement with those seen in Figure 10.

Mathematical curve fitting was performed using CasaXPS software for the XPS analysis on the disk wear surfaces. Iron was fitted based on the presence of three different species, Fe₂O₃ in the 709–711 eV range, FeO in the 707–711 eV range and iron oxy hydroxides (FeOOH) with energies higher than 711 eV. Eventually, iron (0) was searched for at energies below 707.5 eV, but the content was negligible. Fitting was performed using a Gaussian–Lorentzian 70:30 curve for FeO and FeOOH, whereas a Gaussian–Lorentzian 45:55 with an exponential blend of 1.5 was used for Fe₂O₃. Peak position assignment was carried out based on data published in several databases [101,102] and summarized in Table 2.

Table 2. Assignment of binding energies. All energies are expressed in eV.

		From	To
O1s	C=O	532.0	532.2
	C–O	533.3	533.5
	Oxihydroxides	530.9	531.1
	Oxides	529.4	529.7
Fe2p	Fe ₂ O ₃	707.6	710.3
	FeO	710.0	711.2
	FeOOH	712.5	713.4

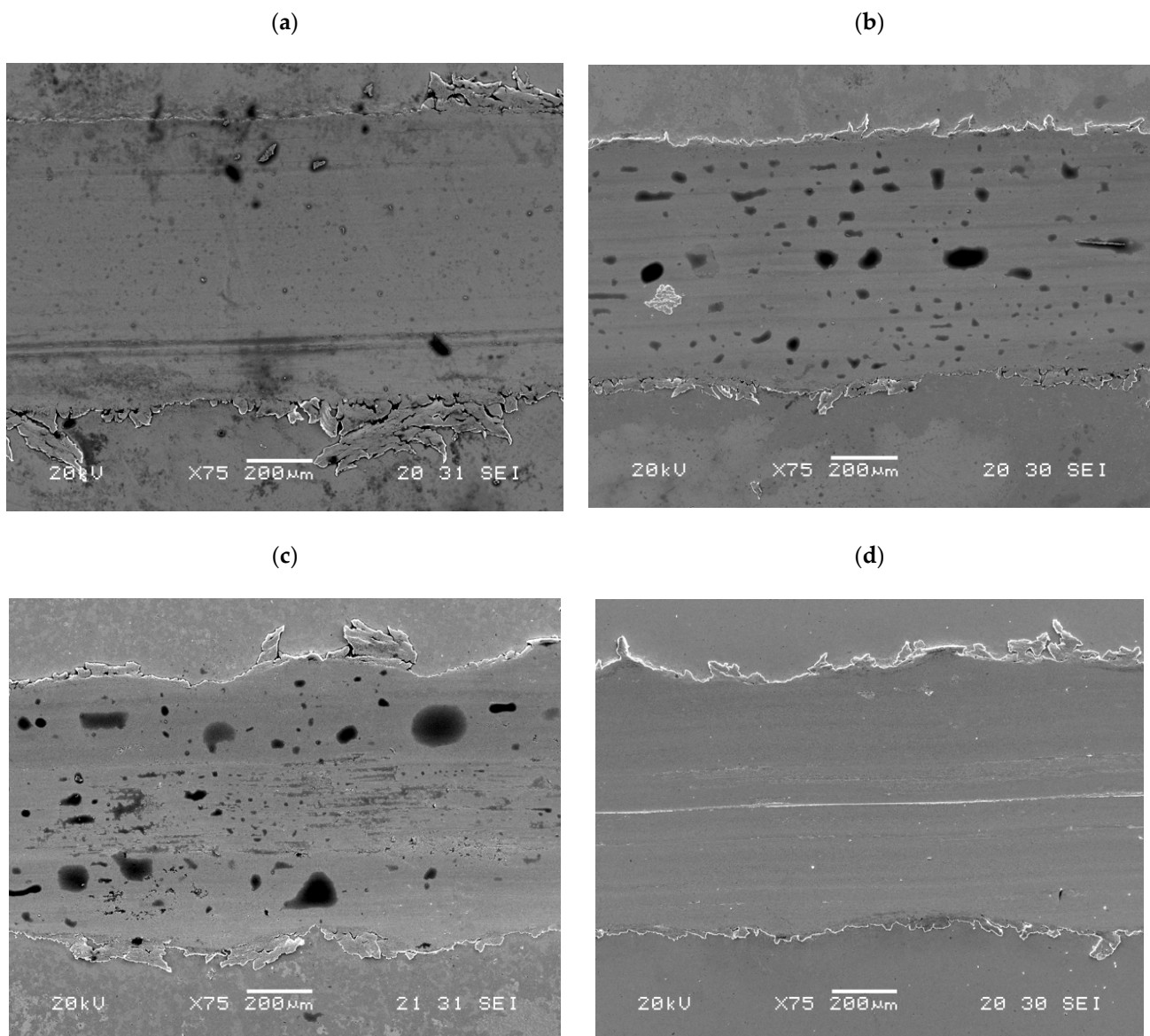


Figure 11. Micrographs of wear scars on the different discs after tribological tests (a) E1, (b) E1 + 2% FAIL, (c) M1 and (d) M1 + 2% FAIL.

The O1s results (Table 3) agreed with the antiwear behavior found after analyzing the wear scars on the disks. An approximately constant amount of organic oxygen (C–O plus C=O), as well as a constant amount of FeOOH + oxides, was found for the base M1 and the blends with the FAIL. On the other hand, the E1 + FAIL blend exhibited a notable increase in organic oxygen with respect to the base oil or, in other words, a reduction in the oxides content.

Table 3. O1s percentage composition.

	Oxides	C–O	FeOOH	C=O
E1	54.66	8.44	20.85	16.05
E1 + 2%FAIL	45.65	13.58	18.75	22.03
M	54.01	7.04	22.6	16.34
M1 + 2%FAIL	57.74	6.99	20.41	14.86

With respect to Fe2p (Table 4), the presence of the ionic liquid seems to have had a reductant effect on the surface when solved in E1 base oil, since the FeO/Fe₂O₃ ratio greatly increased in the presence of FAIL. This effect was not so important in the case of the M1 oil, for which the increase was slight. Likewise, the amounts of surface iron oxy-hydroxides did not seem to undergo large modifications in the presence of FAIL in any of the cases. In fact, although the FeO/Fe₂O₃ ratio changed in some of the samples, the total amount of oxides remained constant, as can be seen from the O1s spectra, since for the two kinds of oxides these spectra are too close to be distinguished.

Table 4. Fe2p percentage composition.

	Fe ₂ O ₃	FeO	FeOOH
E1	62.89	21.77	15.34
E1 + 2%FAIL	10.43	63.55	26.01
M1	25.92	57.22	16.86
M1 + 2%FAIL	19.63	60.47	19.89

The surface composition (Table 5) seemed to indicate a significant organic layer with negligible amounts of nitrogen, thus suggesting a poor interaction with FAIL. Furthermore, the chemical compositions of the worn surface after tests with lubricant samples with and without FAIL were very similar in the case of the E1 oil. However, in the lubricant samples M1 and M1 + FAIL, the presence of the ionic liquid resulted in a lower amount of carbon and a higher amount of oxygen, although the high-resolution spectra of both Fe2p and O1s peaks did not reveal significant differences regarding the chemical state.

Table 5. Surface chemical composition (percentage).

	C	O	N	Fe
E1	72	23	0.2	4.3
E1 + 2%FAIL	76	20	0.2	3.4
M1	70	24	0.5	5.3
M1 + 2%FAIL	60	30	1.0	9.2

4. Conclusions

A novel FAIL obtained via metathesis synthesis was studied as an additive in two different base oils at 2 wt.%. The main conclusions that can be drawn from this work are:

- The FAIL was miscible in the two base oils and no important changes in density and viscosity were found by using it as an additive at 2 wt.% concentration.
- The M1 + FAIL blend showed the highest friction values under the EHL regime and the lowest ones under the ML regime, corresponding to its higher viscosity, which facilitates the formation of a thicker lubricant film at lower speeds. In contrast, the E1 + FAIL showed the lowest friction values under EHL, probably due to its higher polarity and affinity for the metallic surface.
- E1 + FAIL showed a constant increase in the tribofilm thickness during the test, achieving the highest values recorded for the two lubricant samples studied. On the other hand, the M1 + FAIL only registered a very slight increase in tribofilm thickness.
- The E1 + FAIL blend outperformed the antiwear behavior of the base oil, probably due to the better chemical affinity (higher polarity) of this blend for the metallic surface.
- The predominant wear mechanism found after wear tests was of the adhesive type with plastic deformation, and the presence of increasing amounts of organic oxygen (C–O plus C=O) on the wear scar led to better antiwear performance when the E1 + FAIL blend was used.

Author Contributions: Conceptualization, R.G., A.H.-B., P.I. and J.L.V.; Data curation, D.B.; Formal analysis, A.F.-G.; Investigation, J.F., A.F.-G. and J.L.V.; Methodology, R.G. and D.B.; Project administration, R.G. and A.H.-B.; Software, J.F.; Supervision, A.H.-B. and P.I.; Writing—original draft, J.F., R.G. and J.L.V.; Writing—review & editing, A.H.-B., P.I. and J.L.V. All authors have read and agreed to the published version of the manuscript.

Funding: This research was funded by Ministry of Science, Innovation and Universities (Spain), grant number: DPI2016-79690-R (FAILs_LUBEs project). This work was also partially funded by the Foundation for the Promotion of Applied Scientific Research and Technology in Asturias (project LuSuTec. Grant number: IDI/2018/000131).

Data Availability Statement: Data is contained within the article.

Acknowledgments: The authors are grateful to the Ministry of Science, Innovation and Universities of the Spanish government for supporting the research stay of J.L.V. at Rochester Institute of Technology (NY, USA). Grant number: PRX19/00323.

Conflicts of Interest: The authors declare no conflict of interest.

References

1. Walden, P. Molecular weights and electrical conductivity of several fused salts. *Bull. Imp. Acad. Sci.* **1914**, *8*, 405–422.
2. Chum, H.L.; Koch, V.R.; Miller, L.L.; Osteryoung, R.A. Electrochemical scrutiny of organometallic iron complexes and hexamethylbenzene in a room temperature molten salt. *J. Am. Chem. Soc.* **1975**, *97*, 3264–3265. [[CrossRef](#)]
3. Wilkes, J.S.; Levisky, J.A.; Wilson, R.A.; Hussey, C.L. Dialkylimidazolium chloroaluminate melts: A new class of room-temperature ionic liquids for electrochemistry, spectroscopy and synthesis. *Inorg. Chem.* **1982**, *21*, 1263–1264. [[CrossRef](#)]
4. Wilkes, J.S.; Zaworotko, M.J. Air and water stable 1-ethyl-3-methylimidazolium based ionic liquids. *J. Chem. Soc. Chem. Commun.* **1992**, *13*, 965–967. [[CrossRef](#)]
5. Olivier, H. Recent developments in the use of non-aqueous ionic liquids for two-phase catalysis. *J. Mol. Catal. A Chem.* **1999**, *146*, 285–289. [[CrossRef](#)]
6. Wassercheid, P.; Welton, T. *Ionic Liquid in Synthesis*, 2nd ed.; Wiley: Berlin, Germany, 2008.
7. Welton, T. Room-Temperature Ionic Liquids. Solvents for Synthesis and Catalysis. *Chem. Rev.* **1999**, *99*, 2071–2084. [[CrossRef](#)]
8. Hagiwara, R.; Ito, Y. Room temperature ionic liquids of alkylimidazolium cations and fluoroanions. *J. Fluor. Chem.* **2000**, *105*, 221–227. [[CrossRef](#)]
9. Ye, C.F.; Liu, W.M.; Chen, Y.X.; Yu, L.G. Room-temperature ionic liquids: A novel versatile lubricant. *Chem. Commun.* **2001**, *21*, 2244–2245. [[CrossRef](#)]
10. Jiménez, A.E.; Bermúdez, M.D.; Iglesias, P.; Carrión, F.J.; Martínez-Nicolás, G. 1-N-alkyl-3-methylimidazolium ionic liquids as neat lubricants and lubricant additives in steel–aluminium contacts. *Wear* **2006**, *260*, 766–782. [[CrossRef](#)]
11. Iglesias, P.; Bermúdez, M.D.; Carrión, F.J.; Martínez-Nicolás, G. Friction and wear of aluminium–steel contacts lubricated with ordered fluids-neutral and ionic liquid crystals as oil additives. *Wear* **2004**, *256*, 386–392. [[CrossRef](#)]
12. Wang, H.; Lu, Q.; Ye, C.; Liu, W.; Cui, Z. Friction and wear behaviors of ionic liquid of alkylimidazolium hexafluorophosphates as lubricants for steel/steel contact. *Wear* **2004**, *256*, 44–48. [[CrossRef](#)]
13. Imran; Amanullah. Phosphorus and Boron Application Optimizing Biofortification of P and Productivity of French Bean (*Phaseolus vulgaris* L.). *Commun. Soil Sci. Plant Anal.* **2021**, *52*, 2876–2883. [[CrossRef](#)]
14. Cigno, E.; Magagnoli, C.; Pierce, M.; Iglesias, P. Lubricating ability of two phosphonium-based ionic liquids as additives of a bio-oil for use in wind turbines gearboxes. *Wear* **2017**, *376–377*, 756–765. [[CrossRef](#)]
15. Qu, J.; Truhan, J.J.; Dai, S.; Luo, H.; Blau, P.J. Ionic liquids with ammonium cations as lubricants or additives. *Tribol. Lett.* **2006**, *22*, 207–214. [[CrossRef](#)]
16. Kamimura, H.; Kubo, T.; Minami, I.; Mori, S. Effect and mechanism of additives for ionic liquids as new lubricants. *Tribol. Int.* **2007**, *40*, 620–625. [[CrossRef](#)]
17. Fox, M.F.; Priest, M. Tribological properties of ionic liquids as lubricants and additives. Part 1: Synergistic tribofilm formation between ionic liquids and tricresyl phosphate. *Proc. Inst. Mech. Eng. J J. Eng. Tribol.* **2008**, *222*, 291–303. [[CrossRef](#)]
18. Minami, I. Ionic Liquids in Tribology. *Molecules* **2009**, *14*, 2286–2305. [[CrossRef](#)] [[PubMed](#)]
19. Bermúdez, M.D.; Jiménez, A.-E.; Sanes, J.; Carrión, F.-J. Ionic Liquids as Advanced Lubricant Fluids. *Molecules* **2009**, *14*, 2888–2908. [[CrossRef](#)] [[PubMed](#)]
20. Matczak, L.; Johanning, C.; Gil, E.; Guo, H.; Smith, T.W.; Schertzer, M.; Iglesias, P. Effect of cation nature on the lubricating and physicochemical properties of three ionic liquids. *Tribol. Int.* **2018**, *124*, 23–33. [[CrossRef](#)]
21. Zhou, F.; Liang, Y.; Liu, W. Ionic liquid lubricants: Designed chemistry for engineering applications. *Chem. Soc. Rev.* **2009**, *38*, 2590–2599. [[CrossRef](#)]
22. Fraser, K.J.; Macfarlane, D.R. Phosphonium-Based Ionic Liquids: An Overview. *Aust. J. Chem.* **2009**, *62*, 309–321. [[CrossRef](#)]
23. Palacio, M.; Bhushan, B. A Review of Ionic Liquids for Green Molecular Lubrication in Nanotechnology. *Tribol. Lett.* **2010**, *40*, 247–268. [[CrossRef](#)]

24. Somers, A.E.; Howlett, P.C.; Macfarlane, D.R.; Forsyth, M. A Review of Ionic Liquid Lubricants. *Lubricants* **2013**, *1*, 3–21. [[CrossRef](#)]
25. Otero, I.; López, E.R.; Reichelt, M.; Villanueva, M.; Salgado, J.; Fernández, J. Ionic Liquids Based on Phosphonium Cations As Neat Lubricants or Lubricant Additives for a Steel/Steel Contact. *ACS Appl. Mater. Interfaces* **2014**, *6*, 13115–13128. [[CrossRef](#)] [[PubMed](#)]
26. Sharma, V.; Gabler, C.; Doerr, N.; Aswath, P.B. Mechanism of tribofilm formation with P and S containing ionic liquids. *Tribol. Int.* **2015**, *92*, 353–364. [[CrossRef](#)]
27. Battez, A.E.H.; Bartolome, M.; Blanco, D.; Viesca, J.L.; Fernández-González, A.; González, R. Phosphonium cation-based ionic liquids as neat lubricants: Physicochemical and tribological performance. *Tribol. Int.* **2016**, *95*, 118–131. [[CrossRef](#)]
28. Xiao, H. Ionic Liquid Lubricants: Basics and Applications. *Tribol. Trans.* **2016**, *60*, 20–30. [[CrossRef](#)]
29. Battez, A.H.; Fernandes, C.M.; Martins, R.C.; Graça, B.M.; Anand, M.; Blanco, D.; Seabra, J.H. Two phosphonium cation-based ionic liquids used as lubricant additive. Part II: Tribofilm analysis and friction torque loss in cylindrical roller thrust bearings at constant temperature. *Tribol. Int.* **2017**, *109*, 496–504. [[CrossRef](#)]
30. Battez, A.H.; Fernandes, C.M.; Martins, R.C.; Bartolomé, M.; González, R.; Seabra, J.H. Two phosphonium cation-based ionic liquids used as lubricant additive. *Tribol. Int.* **2016**, *107*, 233–239. [[CrossRef](#)]
31. Zhao, D.; Liao, Y.; Zhang, Z. Toxicity of Ionic Liquids. *CLEAN—Soil Air Water* **2007**, *35*, 42–48. [[CrossRef](#)]
32. Pretti, C.; Chiappe, C.; Baldetti, I.; Brunini, S.; Monni, G.; Intorre, L. Acute toxicity of ionic liquids for three freshwater organisms: *Pseudokirchneriella subcapitata*, *Daphnia magna* and *Danio rerio*. *Ecotoxicol. Environ. Saf.* **2009**, *72*, 1170–1176. [[CrossRef](#)] [[PubMed](#)]
33. Ventura, S.P.; Marques, C.S.; Rosatella, A.A.; Afonso, C.A.; Gonçalves, F.; Coutinho, J.A. Toxicity assessment of various ionic liquid families towards *Vibrio fischeri* marine bacteria. *Ecotoxicol. Environ. Saf.* **2012**, *76*, 162–168. [[CrossRef](#)] [[PubMed](#)]
34. Ben Ghanem, O.; Papaiconomou, N.; Mutalib, M.A.; Viboud, S.; El-Harbawi, M.; Uemura, Y.; Gonfa, G.; Bustam, M.A.; Lévêque, J.-M. Thermophysical properties and acute toxicity towards green algae and *Vibrio fischeri* of amino acid-based ionic liquids. *J. Mol. Liq.* **2015**, *212*, 352–359. [[CrossRef](#)]
35. Salgado, J.; Parajó, J.; Teixeira, T.; Cruz, O.; Proupín, J.; Villanueva, M.; Rodríguez-Añón, J.; Verdes, P.; Reyes, O. New insight into the environmental impact of two imidazolium ionic liquids. Effects on seed germination and soil microbial activity. *Chemosphere* **2017**, *185*, 665–672. [[CrossRef](#)] [[PubMed](#)]
36. Predel, T.; Schlücker, E.; Wasserscheid, P.; Gerhard, D.; Arlt, W. Ionic Liquids as Operating Fluids in High Pressure Applications. *Chem. Eng. Technol.* **2007**, *30*, 1475–1480. [[CrossRef](#)]
37. Nainaparampil, J.J.; Eapen, K.C.; Sanders, J.H.; Voevodin, A. Ionic-liquid lubrication of sliding MEMS contacts: Comparison of AFM liquid cell and device-level tests. *J. Microelectromech. Syst.* **2007**, *16*, 836–843. [[CrossRef](#)]
38. Street, K.W.; Morales, W.; Koch, V.R.; Valco, D.J.; Richard, R.M.; Hanks, N. Evaluation of Vapor Pressure and Ultra-High Vacuum Tribological Properties of Ionic Liquids. *Tribol. Trans.* **2011**, *54*, 911–919. [[CrossRef](#)]
39. Mo, Y.; Huang, F.; Zhao, F. Functionalized imidazolium wear-resistant ionic liquid ultrathin films for MEMS/NEMS applications. *Surf. Interface Anal.* **2010**, *43*, 1006–1014. [[CrossRef](#)]
40. Zhang, S.; Hu, L.; Qiao, D.; Feng, D.; Wang, H. Vacuum tribological performance of phosphonium-based ionic liquids as lubricants and lubricant additives of multialkylatedcyclopentanes. *Tribol. Int.* **2013**, *66*, 289–295. [[CrossRef](#)]
41. Jiang, D.; Hu, L.; Feng, D. Tribological properties of crown-type phosphate ionic liquids as lubricating additives in rapeseed oils. *Lubr. Sci.* **2012**, *25*, 195–207. [[CrossRef](#)]
42. García, A.; González, R.; Battez, A.E.H.; Viesca, J.L.; Monge, R.; Fernández-González, A.; Hadfield, M. Ionic liquids as a neat lubricant applied to steel–steel contacts. *Tribol. Int.* **2014**, *72*, 42–50. [[CrossRef](#)]
43. Jimenez, A.E.; Bermúdez, M.D.; Carrión, F.J.; Martínez-Nicolás, G. Room temperature ionic liquids as lubricant additives in steel–aluminium contacts: Influence of sliding velocity, normal load and temperature. *Wear* **2006**, *261*, 347–359. [[CrossRef](#)]
44. Yu, B.; Bansal, D.G.; Qu, J.; Sun, X.; Luo, H.; Dai, S.; Blau, P.J.; Bunting, B.G.; Mordukhovich, G.; Smolenski, D.J. Oil-miscible and non-corrosive phosphonium-based ionic liquids as candidate lubricant additives. *Wear* **2012**, *289*, 58–64. [[CrossRef](#)]
45. Totolin, V.; Minami, I.; Gabler, C.; Brenner, J.; Dörr, N. Lubrication Mechanism of Phosphonium Phosphate Ionic Liquid Additive in Alkylborane–Imidazole Complexes. *Tribol. Lett.* **2014**, *53*, 421–432. [[CrossRef](#)]
46. González, R.; Bartolomé, M.; Blanco, D.; Viesca, J.L.; Fernández-González, A.; Battez, A.E.H. Effectiveness of phosphonium cation-based ionic liquids as lubricant additive. *Tribol. Int.* **2016**, *98*, 82–93. [[CrossRef](#)]
47. Zhou, Y.; Qu, J. Ionic Liquids as Lubricant Additives: A Review. *ACS Appl. Mater. Interfaces* **2017**, *9*, 3209–3222. [[CrossRef](#)] [[PubMed](#)]
48. Sanes, J.; Avilés, M.-D.; Saurín, N.; Espinosa, T.; Carrión, F.-J.; Bermúdez, M.-D. Synergy between graphene and ionic liquid lubricant additives. *Tribol. Int.* **2017**, *116*, 371–382. [[CrossRef](#)]
49. Wang, Y.; Yu, Q.; Cai, M.; Shi, L.; Zhou, F.; Liu, W. Ibuprofen-Based Ionic Liquids as Additives for Enhancing the Lubricity and Antiwear of Water–Ethylene Glycol Liquid. *Tribol. Lett.* **2017**, *65*, 55. [[CrossRef](#)]
50. Viesca, J.L.; Mallada, M.; Blanco, D.; Fernández-González, A.; Casado, J.E.; González, R.; Battez, A.H. Lubrication performance of an ammonium cation-based ionic liquid used as an additive in a polar oil. *Tribol. Int.* **2017**, *116*, 422–430. [[CrossRef](#)]
51. Huang, G.; Yu, Q.; Ma, Z.; Cai, M.; Zhou, F.; Liu, W. Oil-soluble ionic liquids as antiwear and extreme pressure additives in poly- α -olefin for steel/steel contacts. *Friction* **2017**, *7*, 18–31. [[CrossRef](#)]

52. Guangteng, G.; Spikes, H. Fractionation of liquid lubricants at solid surfaces. *Wear* **1996**, *200*, 336–345. [[CrossRef](#)]
53. Rico, J.F.; Battez, A.H.; Cuervo, D.G. Wear prevention characteristics of binary oil mixtures. *Wear* **2002**, *253*, 827–831. [[CrossRef](#)]
54. Cambiella, A.; Benito, J.M.; Pazos, C.; Coca, J.; Hernández, A.; Fernández, J.E. Formulation of emulsifiable cutting fluids and extreme pressure behaviour. *J. Mater. Process. Technol.* **2007**, *184*, 139–145. [[CrossRef](#)]
55. Battez, A.E.H.; González, R.; Viesca, J.L.; Blanco, D.; Asedegbega, E.; Osorio, A. Tribological behaviour of two imidazolium ionic liquids as lubricant additives for steel/steel contacts. *Wear* **2009**, *266*, 1224–1228. [[CrossRef](#)]
56. Mistry, K.; Fox, M.F.; Priest, M. Lubrication of an electroplated nickel matrix silicon carbide coated eutectic aluminium—Silicon alloy automotive cylinder bore with an ionic liquid as a lubricant additive. *Proc. Inst. Mech. Eng. J J. Eng. Tribol.* **2009**, *223*, 563–569. [[CrossRef](#)]
57. Lu, R.; Nanao, H.; Kobayashi, K.; Kubo, T.; Mori, S. Effect of Lubricant Additives on Tribochemical Decomposition of Hydrocarbon Oil on Nascent Steel Surfaces. *J. Jpn. Pet. Inst.* **2010**, *53*, 55–60. [[CrossRef](#)]
58. Blanco, D.; Battez, A.E.H.; Viesca, J.L.; González, R.; Fernández-González, A. Lubrication of CrN Coating With Ethyl-Dimethyl-2-Methoxyethylammonium Tris(pentafluoroethyl)Trifluorophosphate Ionic Liquid as Additive to PAO 6. *Tribol. Lett.* **2011**, *41*, 295–302. [[CrossRef](#)]
59. Blanco, D.; González, R.; Battez, A.H.; Viesca, J.L.; Fernández-González, A. Use of ethyl-dimethyl-2-methoxyethylammonium tris(pentafluoroethyl)trifluorophosphate as base oil additive in the lubrication of TiN PVD coating. *Tribol. Int.* **2011**, *44*, 645–650. [[CrossRef](#)]
60. Cai, M.; Liang, Y.; Yao, M.; Xia, Y.; Zhou, F.; Liu, W. Imidazolium Ionic Liquids as Antiwear and Antioxidant Additive in Poly(ethylene glycol) for Steel/Steel Contacts. *ACS Appl. Mater. Interfaces* **2010**, *2*, 870–876. [[CrossRef](#)]
61. Jiménez, A.-E.; Bermúdez, M.-D. Short alkyl chain imidazolium ionic liquid additives in lubrication of three aluminium alloys with synthetic ester oil. *Tribol.—Mater. Surf. Interfaces* **2012**, *6*, 109–115. [[CrossRef](#)]
62. Somers, A.E.; Khemchandani, B.; Howlett, P.C.; Sun, J.; MacFarlane, D.R.; Forsyth, M. Ionic Liquids as Antiwear Additives in Base Oils: Influence of Structure on Miscibility and Antiwear Performance for Steel on Aluminum. *ACS Appl. Mater. Interfaces* **2013**, *5*, 11544–11553. [[CrossRef](#)] [[PubMed](#)]
63. Cai, M.; Liang, Y.; Zhou, F.; Liu, W. A novel imidazolium salt with antioxidation and anticorrosion dual functionalities as the additive in poly(ethylene glycol) for steel/steel contacts. *Wear* **2013**, *306*, 197–208. [[CrossRef](#)]
64. Qiao, D.; Wang, H.; Feng, D. Tribological Performance and Mechanism of Phosphate Ionic Liquids as Additives in Three Base Oils for Steel-on-aluminum Contact. *Tribol. Lett.* **2014**, *55*, 517–531. [[CrossRef](#)]
65. Kronberger, M.; Pagano, F.; Pejaković, V.; Igartua, A.; Urbistondo, E.; Kalin, M. Miscibility and tribological investigations of ionic liquids in biodegradable esters. *Lubr. Sci.* **2014**, *26*, 463–487. [[CrossRef](#)]
66. Gusain, R.; Gupta, P.; Saran, S.; Khatri, O.P. Halogen-Free Bis(imidazolium)/Bis(ammonium)-Di[bis(salicylato)borate] Ionic Liquids as Energy-Efficient and Environmentally Friendly Lubricant Additives. *ACS Appl. Mater. Interfaces* **2014**, *6*, 15318–15328. [[CrossRef](#)]
67. Zhu, L.; Zhao, Q.; Wu, X.; Zhao, G.; Wang, X. A novel phosphate ionic liquid plays dual role in synthetic ester oil: From synthetic catalyst to anti-wear additive. *Tribol. Int.* **2016**, *97*, 192–199. [[CrossRef](#)]
68. Qiu, X.; Lu, L.; Qu, Z.; Liao, J.; Fan, Q.; Shah, F.U.; Zhang, W.; An, R. Probing the nanofriction of non-halogenated phosphonium-based ionic liquid additives in glycol ether oil on titanium surface. *Friction* **2022**, *10*, 268–281. [[CrossRef](#)]
69. Blanco, D.; González, R.; Viesca, J.L.; Fernández-González, A.; Bartolomé, M.; Battez, A.H. Antifriction and Antiwear Properties of an Ionic Liquid with Fluorine-Containing Anion Used as Lubricant Additive. *Tribol. Lett.* **2017**, *65*, 66. [[CrossRef](#)]
70. Battez, A.H.; Ramos, D.; Blanco, D.; González, R.; Fernández-González, A.; Viesca, J.L. Lubrication Properties of the Ionic Liquid Dodecyl-3 Methylimidazolium bis(trifluoromethylsulfonyl)imide. *Tribol. Lett.* **2017**, *66*, 19. [[CrossRef](#)]
71. González, R.; Ramos, D.; Blanco, D.; Viesca, J.L.; Hadfield, M.; Battez, A.H. Tribological performance of tributylmethylammonium bis (trifluoromethylsulfonyl) amide as neat lubricant and as an additive in a polar oil. *Friction* **2019**, *7*, 282–288. [[CrossRef](#)]
72. Willing, A. Lubricants based on renewable resources—An environmentally compatible alternative to mineral oil products. *Chemosphere* **2001**, *43*, 89–98. [[CrossRef](#)]
73. Mannekote, J.K.; Menezes, P.L.; Kailas, S.V.; Sathwik, R.K.C. Tribology of Green Lubricants. In *Tribology Scientists and Engineers*; Springer: New York, NY, USA, 2013; pp. 495–521.
74. Holmberg, K.; Erdemir, A. Influence of tribology on global energy consumption, costs and emissions. *Friction* **2017**, *5*, 263–284. [[CrossRef](#)]
75. Guo, H.; Iglesias, P. Tribological behavior of ammonium-based protic ionic liquid as lubricant additive. *Friction* **2021**, *9*, 169–178. [[CrossRef](#)]
76. Yu, Q.; Zhang, C.; Dong, R.; Shi, Y.; Wang, Y.; Bai, Y.; Zhang, J.; Cai, M.; Zhou, F.; Liu, W. Physicochemical and tribological properties of gemini-type halogen-free dicationic ionic liquids. *Friction* **2021**, *9*, 344–355. [[CrossRef](#)]
77. Costa, S.P.F.; Azevedo, A.M.O.; Pinto, P.C.A.G.; Saraiva, M.L.M.F.S. Environmental Impact of Ionic Liquids: Recent Advances in (Eco)toxicology and (Bio)degradability. *ChemSusChem* **2017**, *10*, 2321–2347. [[CrossRef](#)]
78. Adawiyah, N.; Hawatulaila, S.; Aini, A.; Vijaya, A.; Ibrahim, M.; Moniruzzaman, M. Synthesis, characterization, ecotoxicity and biodegradability evaluations of novel biocompatible surface active lauroyl sarcosinate ionic liquids. *Chemosphere* **2019**, *229*, 349–357. [[CrossRef](#)]

79. Parmentier, D.; Metz, S.J.; Kroon, M.C. Tetraalkylammonium oleate and linoleate based ionic liquids: Promising extractants for metal salts. *Green Chem.* **2012**, *15*, 205–209. [[CrossRef](#)]
80. Rocha, M.A.A.; Bruinhorst, A.V.D.; Schröer, W.; Rathke, B.; Kroon, M.C. Physicochemical properties of fatty acid based ionic liquids. *J. Chem. Thermodyn.* **2016**, *100*, 156–164. [[CrossRef](#)]
81. Gusain, R.; Dhingra, S.; Khatri, O.P. Fatty-Acid-Constituted Halogen-Free Ionic Liquids as Renewable, Environmentally Friendly, and High-Performance Lubricant Additives. *Ind. Eng. Chem. Res.* **2016**, *55*, 856–865. [[CrossRef](#)]
82. Gusain, R.; Khatri, O.P. Fatty acid ionic liquids as environmentally friendly lubricants for low friction and wear. *RSC Adv.* **2016**, *6*, 3462–3469. [[CrossRef](#)]
83. Mezzetta, A.; Guazzelli, L.; Seggiani, M.; Pomelli, C.S.; Puccini, M.; Chiappe, C. A general environmentally friendly access to long chain fatty acid ionic liquids (LCFA-ILs). *Green Chem.* **2017**, *19*, 3103–3111. [[CrossRef](#)]
84. Fan, M.; Ma, L.; Zhang, C.; Wang, Z.; Ruan, J.; Han, M.; Ren, Y.; Zhang, C.; Yang, D.; Zhou, F.; et al. Biobased Green Lubricants: Physicochemical, Tribological and Toxicological Properties of Fatty Acid Ionic Liquids. *Tribol. Trans.* **2017**, *61*, 195–206. [[CrossRef](#)]
85. Khatri, P.K.; Aathira, M.S.; Thakre, G.D.; Jain, S.L. Synthesis and tribological behavior of fatty acid constituted tetramethylguanidinium (TMG) ionic liquids for a steel/steel contact. *Mater. Sci. Eng. C* **2018**, *91*, 208–217. [[CrossRef](#)] [[PubMed](#)]
86. Zheng, G.; Ding, T.; Huang, Y.; Zheng, L.; Ren, T. Fatty acid based phosphite ionic liquids as multifunctional lubricant additives in mineral oil and refined vegetable oil. *Tribol. Int.* **2018**, *123*, 316–324. [[CrossRef](#)]
87. Blanco, D.; Rivera, N.; Oulego, P.; Díaz, M.; González, R.; Battez, A.H. Novel fatty acid anion-based ionic liquids: Contact angle, surface tension, polarity fraction and spreading parameter. *J. Mol. Liq.* **2019**, *288*, 110995. [[CrossRef](#)]
88. Rivera, N.; Blanco, D.; Viesca, J.L.; Fernández-González, A.; González, R.; Battez, A.H. Tribological performance of three fatty acid anion-based ionic liquids (FAILs) used as lubricant additive. *J. Mol. Liq.* **2019**, *296*, 111881. [[CrossRef](#)]
89. Khan, A.; Gusain, R.; Sahai, M.; Khatri, O.P. Fatty acids-derived protic ionic liquids as lubricant additive to synthetic lube base oil for enhancement of tribological properties. *J. Mol. Liq.* **2019**, *293*, 111444. [[CrossRef](#)]
90. Rivera, N.; García, A.; Fernández-González, A.; Blanco, D.; González, R.; Battez, A.H. Tribological behavior of three fatty acid ionic liquids in the lubrication of different material pairs. *J. Mol. Liq.* **2019**, *296*, 111858. [[CrossRef](#)]
91. Ali, K.; Moshikur, R.; Wakabayashi, R.; Tahara, Y.; Moniruzzaman, M.; Kamiya, N.; Goto, M. Synthesis and characterization of choline–fatty-acid-based ionic liquids: A new biocompatible surfactant. *J. Colloid Interface Sci.* **2019**, *551*, 72–80. [[CrossRef](#)]
92. Oulego, P.; Faes, J.; Gonzalez, R.; Viesca, J.L.; Blanco, D.; Battez, A.H. Relationships between the physical properties and biodegradability and bacteria toxicity of fatty acid-based ionic liquids. *J. Mol. Liq.* **2019**, *292*, 111451. [[CrossRef](#)]
93. Gundolf, T.; Weyhing-Zerrer, N.; Sommer, J.; Kalb, R.; Schoder, D.; Rossmannith, P.; Mester, P. Biological Impact of Ionic Liquids Based on Sustainable Fatty Acid Anions Examined with a Tripartite Test System. *ACS Sustain. Chem. Eng.* **2019**, *7*, 15865–15873. [[CrossRef](#)]
94. Gusain, R.; Khan, A.; Khatri, O.P. Fatty acid-derived ionic liquids as renewable lubricant additives: Effect of chain length and unsaturation. *J. Mol. Liq.* **2019**, *301*, 112322. [[CrossRef](#)]
95. Sernaglia, M.; Blanco, D.; Battez, A.H.; Viesca, J.L.; González, R.; Bartolomé, M. Two fatty acid anion-based ionic liquids—part I: Physicochemical properties and tribological behavior as neat lubricants. *J. Mol. Liq.* **2020**, *305*, 112827. [[CrossRef](#)]
96. Sernaglia, M.; Blanco, D.; Battez, A.H.; González, R.; Fernández-González, A.; Bartolomé, M. Two fatty acid anion-based ionic liquids—Part II: Effectiveness as an additive to a polyol ester. *J. Mol. Liq.* **2020**, *310*, 113158. [[CrossRef](#)]
97. Faes, J.; González, R.; Battez, A.H.; Blanco, D.; Fernández-González, A.; Viesca, J.L. Friction, Wear and Corrosion Behavior of Environmentally-Friendly Fatty Acid Ionic Liquids. *Coatings* **2021**, *11*, 21. [[CrossRef](#)]
98. Viesca, J.; Faes, J.; Rivera, N.; Rodríguez, E.; Cadenas, M.; González, R. Thermal stability, traction and tribofilm formation of three fatty acid-derived ionic liquids. *Tribol. Int.* **2021**, *154*, 106712. [[CrossRef](#)]
99. Battez, A.E.H.; Rivera, N.; Blanco, D.; Oulego, P.; Viesca, J.L.; González, R. Physicochemical, traction and tribofilm formation properties of three octanoate-, laurate- and palmitate-anion based ionic liquids. *J. Mol. Liq.* **2019**, *284*, 639–646. [[CrossRef](#)]
100. Kapadia, R.; Glyde, R.; Wu, Y. In situ observation of phosphorous and non-phosphorous antiwear films using a mini traction machine with spacer layer image mapping. *Tribol. Int.* **2007**, *40*, 1667–1679. [[CrossRef](#)]
101. National Institute of Standards and Technology (NIST). Available online: https://srdata.nist.gov/xps/main_search_menu.aspx (accessed on 26 February 2022).
102. Thermo Scientific XPS: Knowledge Base. Available online: <https://xpssimplified.com/> (accessed on 26 February 2022).